Cell Wall Maturation of Arabidopsis Trichomes Is Dependent on Exocyst Subunit EXO70H4 and Involves Callose Deposition[1][OPEN]

Ivan Kulich[2]*, Zdeňka Vojtíková[2], Matouš Glanc, Jitka Ortmannová, Sergio Rasmann[3], and Viktor Žárský

Department of Experimental Plant Biology, Faculty of Sciences, Charles University, 12844 Prague, Czech Republic (I.K., Z.V., M.G., J.O., V.Z.); Institute of Experimental Botany, Academy of Sciences of the Czech Republic, 16502 Prague, Czech Republic (J.O., V.Z.); and Department of Ecology and Evolution, University of Lausanne, CH–1015 Lausanne, Switzerland (S.R.)

Arabidopsis (*Arabidopsis thaliana*) leaf trichomes are single-cell structures with a well-studied development, but little is understood about their function. Developmental studies focused mainly on the early shaping stages, and little attention has been paid to the maturation stage. We focused on the EXO70H4 exocyst subunit, one of the most up-regulated genes in the mature trichome. We uncovered EXO70H4-dependent development of the secondary cell wall layer, highly autofluorescent and callose rich, deposited only in the upper part of the trichome. The boundary is formed between the apical and the basal parts of mature trichome by a callose ring that is also deposited in an EXO70H4-dependent manner. We call this structure the Ortmannian ring (OR). Both the secondary cell wall layer and the OR are absent in the *exo70H4* mutants. Ecophysiological aspects of the trichome cell wall thickening include interference with antiherbivore defense and heavy metal accumulation. Ultraviolet B light induces EXO70H4 transcription in a CONSTITUTIVE PHOTOMORPHOGENIC1-dependent way, resulting in stimulation of trichome cell wall thickening and the OR biogenesis. EXO70H4-dependent trichome cell wall hardening is a unique phenomenon, which may be conserved among a variety of the land plants. Our analyses support a concept that Arabidopsis trichome is an excellent model to study molecular mechanisms of secondary cell wall deposition.

Driven by selection pressure on reproductive success, the surface layers of land plants continually evolve to endure biotic and abiotic stresses. This has resulted in the dynamic evolution of different epidermis and derived structures, such as trichomes, across species and genotypes. Trichomes particularly can be of different forms, even within one individual plant. Because they are unessential for plant survival in laboratory conditions, trichomes became popular targets of genetic developmental analyses in the model plant Arabidopsis (*Arabidopsis thaliana*); until now, the focus was mostly on trichomes patterning/initiation and early morphogenetic processes. Nevertheless, trichome development has been shown to be modulated by abiotic stresses in Arabidopsis and other systems. Yamasaki et al. (2007), for instance, showed that UV-B irradiation was responsible for increasing the number of cells and the amount of polyphenolic compounds in trichomes. Roles in the drought and heat stresses (Ehleringer, 1982; Grammatikopoulos and Manetas, 1994; Espigares and Peco, 1995; Pérez-Estrada et al., 2000) and heavy metal detoxification and deposition (Salt et al., 1995; Pérez-Estrada et al., 2000; Servin et al., 2012; Jr and Kupper, 2014) also have been described. Additionally, different forms of trichomes have been linked to increased plant resistance against herbivores across different species of plants (for review, see Riddick and Simmons, 2014).

Arabidopsis trichomes are nonglandular hairs with epidermal origin. Unlike most plants with multicellular trichomes, Arabidopsis trichomes are unicellular (but undergo four endoreduplication cycles; Hülskamp et al., 1994). Despite unicellularity, Arabidopsis trichomes reach an extremely polarized shape, with bulged stalk and three to four branches. Development has been well characterized genetically (Hülskamp et al., 1994; Folkers et al., 1997; for review, see Marks et al., 1991), and it has been divided into six stages: initiation, polar expansion, branching, branch growth, diffuse growth, and maturation of cell wall (Szymanski et al., 1998, 2000). Nevertheless, interest has remained firmly focused on the first five stages, when trichome growth and formation occur, with rather less attention paid to the stage of trichome maturation. Only a few mutants with defective trichome maturation have been identified to date. For instance, the

[1] This work was supported by the Grant Agency of Czech Republic (grant no. 14–27329P), the Grant Agency of Charles University (grant no. 658112), the Czech Ministry of Education (grant no. NPUI LO1417), and the City of Prague (grant no. OPPK CZ.2. 16/3.1.00/24014 for the transmission electron microscope used in this study).

[2] These authors contributed equally to the article.

[3] Present address: Institute of Biology, University of Neuchâtel, CH–2000 Neuchâtel, Switzerland.

* Address correspondence to kulich@natur.cuni.cz.

The author responsible for distribution of materials integral to the findings presented in this article in accordance with the policy described in the Instructions for Authors (www.plantphysiol.org) is: Ivan Kulich (kulich@natur.cuni.cz).

[OPEN] Articles can be viewed without a subscription.

www.plantphysiol.org/cgi/doi/10.1104/pp.15.00112

group of glassy mutants lacks surface papillae, rendering them a lustrous and transparent appearance. These include *chablis*, *chardonnay*, *retsina* (Hülskamp et al., 1994), *glassy hair1* (*GLH1*), *GLH2*, *GLH3*, *GLH4*, and *GLH6* (Suo et al., 2013). Unfortunately, only phenotype description and chromosomal position mapping of glassy genes have been published. A similar situation prevails with mutant *underdeveloped trichome* (Haughn and Somerville, 1988) and *constitutive expression of PR genes5* (Brininstool et al., 2008). Mapped mutations affecting the trichome cell wall include several transcription factors and cell wall enzymes. *murus2* mutation is in the fucosyltransferase1, resulting in underdeveloped trichome papillae (Vanzin et al., 2002), similar to *murus3* mutation in the xyloglucan galactosyltransferase (Madson et al., 2003). Mutants named *trichome birefringence* lack the birefringence of the trichomes, which is primarily caused by paracrystalline cellulose. The precise role of these proteins is, however, still unclear (Potikha and Delmer, 1995; Bischoff et al., 2010). Transcription factors involved in the trichome cell wall development include HOMEODOMAIN GLABROUS2 (Marks et al., 2009) and MYB DOMAIN PROTEIN106 (NOECK; Jakoby et al., 2008). Both of these mutants also have underdeveloped trichome papillae.

Only recently has the potential of Arabidopsis trichomes as a model for cell wall biogenesis been recognized (Suo et al., 2013). In fact, most of the published work on cell walls formation was done on stem/xylem or whole-plant analysis and is related to cell wall component biosynthesis (Liepman et al., 2010), with recent emphasis on transcriptional networks reconstructed from transcriptional analyses (Wang et al., 2012).

Exocytosis is a constituent process in cell wall formation, and we are interested in how delivery/targeting and tethering of secretory vesicles to the plasma membrane are involved in Arabidopsis trichome cell wall maturation. Exocyst is an evolutionarily conserved protein complex in all eukaryotes and plays an important role in polarized exocytosis (Elias et al., 2003; Munson and Novick, 2006; Cvrčková et al., 2012). The exocyst complex consists of eight subunits (SEC3, SEC5, SEC6, SEC8, SEC10, SEC15, EXO70, and EXO84). Although it has been initially described in yeast (*Saccharomyces cerevisiae*; TerBush et al., 1996), homologs of all of the subunits have been described in plants (Elias et al., 2003), where they also form a complex (Hála et al., 2008). The role of the exocyst complex is tethering and docking of the post-Golgi vesicles to plasma membrane. SEC3 and EXO70 proteins are believed to be spatial landmarks on the plasma membrane, marking the place of the vesicle fusion (Finger et al., 1998; He et al., 2007). This can be shown by artificial targeting of the SEC3 to the mitochondrial outer membrane, which is followed by relocalization of the remaining exocyst subunits and secretion into the mitochondrion (Luo et al., 2014). The vesicle is attached by the exocyst near to the acceptor target membrane, whereas SNARE proteins mediate the rest of the fusion process. Polarized exocytosis mediated by exocyst enables effective control of growth and final shape of plant cells and tissues. The role of polarized exocytosis in cell wall formation is crucial and makes possible the creation of extremely polarized cells, such as root hairs, or pollen tubes (Cole et al., 2005; Cole and Fowler, 2006; Synek et al., 2006; Zárský et al., 2009).

Interestingly, some of exocyst subunits are found in multiple copies in terrestrial plant genomes (Elias et al., 2003; Hála et al., 2008; Cvrčková et al., 2012). The most protruding is multiplication of subunit EXO70. For example, the genome of *Physcomitrella patens* encodes 13 paralogs of the EXO70 subunit, *Vitis vinifera* encodes 15 paralogs, and *Oryza sativa* encodes 47 paralogs (Cvrčková et al., 2012). The Arabidopsis genome encodes 1 copy of exocyst subunits SEC6 and SEC8, 2 copies of SEC3, SEC5, SEC10, and SEC15, 3 copies of EXO84, and strikingly, 23 copies of EXO70 (Elias et al., 2003; Hála et al., 2008; Cvrčková et al., 2012). It still remains unclear whether the functions of EXO70 paralogs are redundant or specialized, but new findings suggest that at least some EXO70 paralogs have entirely different functions than the most studied and most conserved EXO70A1. Early data show that the transcription of some EXO70 paralogs is up-regulated in specific tissues or under specific conditions. For example, EXO70B2 and EXO70H1 are strongly up-regulated by pathogen elicitors (Pecenkova et al., 2011). Other recent works report the first evidence, to our knowledge, of functional diversification of some EXO70 paralogs, with possible roles in autophagy (Kulich et al., 2013). Formation of other double-membrane bodies has been reported for the EXO70E2 subunit (Wang et al., 2010). Overexpression of EXO70E2 also induces double-membrane structures in animal cells (Ding et al., 2014). This may reflect an exocyst-independent effect of EXO70 on the membrane curvature, which was reported in animal cells (Zhao et al., 2013).

Here, we focus on the EXO70H4 paralog, which is the 11th most up-regulated gene in the mature trichome (Jakoby et al., 2008). Arabidopsis trichomes functions are mostly associated with herbivore defense and UV protection (Yan et al., 2012). Corresponding with this, it was indicated that EXO70H4 is up-regulated by UV-B irradiation in a CONSTITUTIVE PHOTOMORPHOGENIC1 (COP1)-dependent manner (Oravecz et al., 2006) and that it is down-regulated by methyl jasmonate (MeJA; Hruz et al., 2008). MeJA is a volatile plant defense hormone, which is important, especially in response to herbivores and wounding. A recent transcriptome profiling study has identified the cucumber (*Cucumis sativus*) EXO70H4 paralog as also being highly up-regulated during the cucumber fruit trichome development, suggesting that similar mechanisms are present among various land plants (Chen et al., 2014).

In this report, we studied and compared Arabidopsis trichomes maturation between the wild type and *EXO70H4* subunit mutants. Our work has resulted in the description of a component and structure in Arabidopsis trichomes, which we named Ortmannian ring (OR). Additionally, our data highlight that EXO70H4 plays a role in Arabidopsis trichome cell wall maturation

as well as plant response to UV-B irradiation and herbivore attack.

RESULTS

Two Arabidopsis SALK insertional mutants in the *EXO70H4* single-exon gene were used for this study: *exo70H4-1* and *exo70H4-3* (SALK_023593 and SALK_003200, respectively). Annotated position of the insertions was verified by sequencing of the flanking regions. Both lines have transfer DNA insertion in the single exon of the *EXO70H4* gene, and recessive homozygotes exhibit identical phenotypic deviations. *exo70H4-1* has a tandem insertion, disrupting the coding sequence (CDS) 47 bp from the start codon, and *exo70H4-3* has a single insertion, disrupting CDS 580 bp from the start codon (Fig. 1A). According to reverse transcription (RT)-PCR, both mutations prevent synthesis of the full-length RNA, with partial transcripts present (Fig. 1B). Because the phenotypes were identical, most of the following work has been done on the *exo70H4-1* allele. Transformation of the *exo70H4-1* mutant with the genomic fragment, including the promoter (895 bp) and the C-terminal fluorescent marker tagRFP (*Entacmaea quadricolor* red fluorescent protein), has restored the wild-type phenotype of the trichomes (Supplemental Fig. S1).

To test whether EXO70H4 is an exocyst subunit, we performed yeast two-hybrid analysis, which has resulted in interactions with SEC5a, SEC6, and the C terminus of EXO84b and also, a weak interaction with SEC15a (Supplemental Fig. S2).

Overall plant size, structure, and trichome morphogenesis of mutant plants are not affected. However, mutant plants have leaf trichomes that lack rigidity and are more flexible and bendable compared with the wild type. For example, in a blinded study, we were able to precisely distinguish 100% of the mutants from the wild types by touching the leaves (n = 40). This difference is because of the apparently thinner cell walls of mutant trichomes compared with the wild type (Fig. 1C). These observations imply that deposition of cell wall components is defective in *exo70H4* mutants during the trichome maturation phase. At this phase, wild-type trichome cell wall undergoes massive secondary thickening, which progressively fills up trichome inner space. This thickening is mostly pronounced in the branch tips (Fig. 1C) and can be easily measured (Fig. 1D). This extensive deposition results in cytoplasm reduction and recession toward the stalk.

OR, Cell Wall Structure of the Mature Arabidopsis Trichome

During our observation of the trichome cell wall thickening, we noticed a distinct circular thickening of cell wall at the basal region of the stalk (Fig. 1C). This ring, present above the surrounding epidermal cells, appears to divide the trichome into two different domains. Staining with decolorized aniline blue has revealed that the ring is a callose-rich structure (Fig. 2A).

To show that such circular formation is a normal part of Arabidopsis trichome maturation, we captured photographs of whole 24-d-old rosettes stained by aniline blue (Fig. 2B) by automated stitching of individual microscopic frames in three focal depths. With this resolution, we could detect the presence of the callose ring in all leaf trichomes. First, callose rings appear in the oldest trichomes and grow on the apex. Second, a wave of maturation continues, and rings also appear in the leaf base. Because this ring was not studied before, we propose naming it OR after author J.O., who first spotted it.

The OR acts as a boundary and apparently divides the trichome cell wall into two clearly distinct domains—apical (branches and stalk) and basal (bulge). The cell wall in the apical domain shows strong autofluorescence upon UV-B excitation (Fig. 3), it has surface papillae, and it undergoes massive secondary

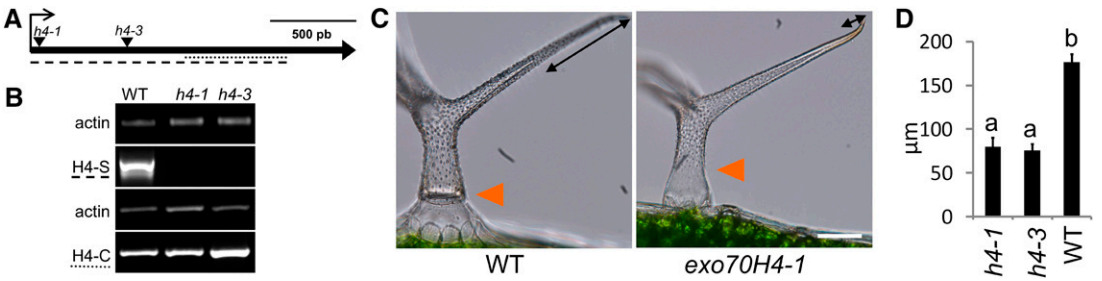

Figure 1. *exo70H4* mutants show trichome cell wall thickening defects. A, Insertions in *exo70H4-1* and *exo70H4-3* mutants disrupt the single exon of *EXO70H4*. B, H4-S and H4-C fragments (shown in A as dashed and dotted lines, respectively) amplified by RT-PCR. C, Phenotypes of the wild type (WT) versus *exo70H4-1* mutant in the trichome tip cell wall (double arrow line) and basal (orange triangle) parts. Bar = 20 μm. D, Quantification of the apical thickening on *exo70H4-1* and *exo70H4-3* mutants. Letters above bars mean significant differences (honestly significant difference [HSD] Tukey post hoc test, $P < 0.01$). Error bars represent SE. Similar results were obtained in three biological replicas.

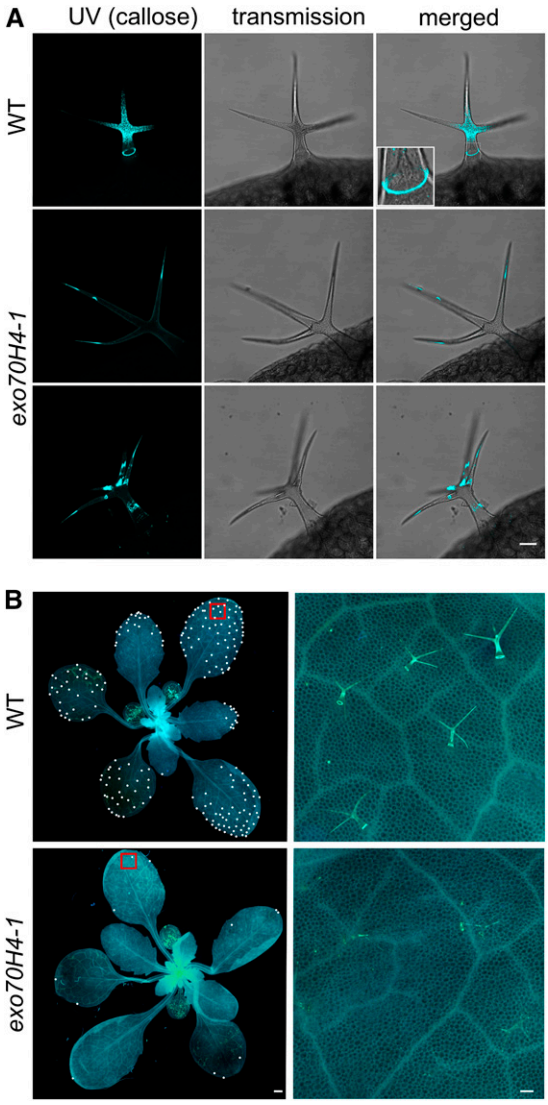

Figure 2. Visualization of the OR. A, Aniline blue staining of the wild type (WT) and *exo70H4-1* mutant. The distinct callose ring is what we termed OR. Bar = 20 μm. B, Whole-rosette aniline blue staining of the 23-d-old wild-type and *exo70H4-1* mutant plants. White dots, Trichomes with the OR already visible; red rectangles, the positions of the zoomed areas. Bars = 1 mm (left); 50 μm (right).

thickening during the maturation phase. In contrast, the basal domain lacks autofluorescence (Fig. 3A) and papillae (Fig. 1C), and its cell wall remains thin. The *exo70H4-1* mutant lacks the OR and most of the callose in the vast majority of the trichomes (more than 95%). *exo70H4-1* trichomes either lack the callose entirely or it can be detected within the cytoplasm in the form of ectopic fibrous bodies (Fig. 2A). No major differences in callose deposition were spotted elsewhere (plasmodesmatal plugs after wounding and vasculature; data not shown). Papillae do develop in the *exo70H4* mutant; however, their distribution is not limited by any clear border area (Fig. 1C).

exo70H4 Mutants Lack a Highly Autofluorescent Internal Cell Wall Layer That Is Bordered by the OR in the Wild Type

In the trichomes of the wild type, the internal cell wall layer can be easily recognized. This layer shows strong autofluorescence, especially upon excitation with 405 nm and emission maxima at 485 nm (Fig. 3B). Interestingly, this high autofluorescence is found only in the upper part of the trichome above the OR (Fig. 3A).

Autofluorescence of the inner cell wall layer is rapidly increased by trichome breakage or damage (Fig. 3, C and D). Because the damaged trichomes were killed by their breakage, gain of autofluorescence was likely caused by oxidation of the inner cell wall layer. This statement is supported by treatment with reducing agents (40 mM mercaptoethanol), which suppressed the autofluorescence buildup after breakage (Fig. 3E). With or without physical damage, *exo70H4* mutants show dramatically decreased autofluorescence compared with the wild type because of the absence of the whole inner cell wall layer. The remaining autofluorescence was more equally distributed within the mutant cell wall (Fig. 3A). The absence of the inner trichome cell wall layer also explains differential calcofluor white (CW) staining of isolated *exo70H4-1* trichome versus the wild type. Whereas in wild-type trichome, only the trichome base was stained, in the mutant, the apical domain was also stained (Supplemental Fig. S3). Hence, the callose-rich inner trichome cell wall layer likely insulates the apical trichome domain and prevents cellulose from staining.

To further characterize EXO70H4-dependent cell wall thickening, we have observed transmission electron microscopy (TEM) sections in isolated trichomes. Our sectioning confirmed that the wild-type trichome contains two clearly distinct cell wall layers—an electron-dense external layer and an internal layer. The internal layer is limited to the apical part of the trichome above the OR, where it forms a bulge of thick cell wall. This second internal cell wall layer is completely absent from *exo70H4* mutant trichomes (Fig. 4, A–D). Immunogold labeling of the callose has revealed that OR is usually U-shaped on cross section bordering the secondary cell wall (Fig. 4, E and F). Results of the immunogold labeling were consistent with aniline blue staining, with callose detected primarily in the OR and less frequently in the secondary cell wall above it. Because the staining was rather weak and specific, we have detected no immunogold particles in the other parts of the section.

By extensive observation of trichomes in different stages of their maturation, we were able to summarize the thickening progress. The secondary cell wall thickening is accompanied by growth of the OR, which is U-shaped on the cross section and widens in the latest stages of the trichome maturation (Fig. 5).

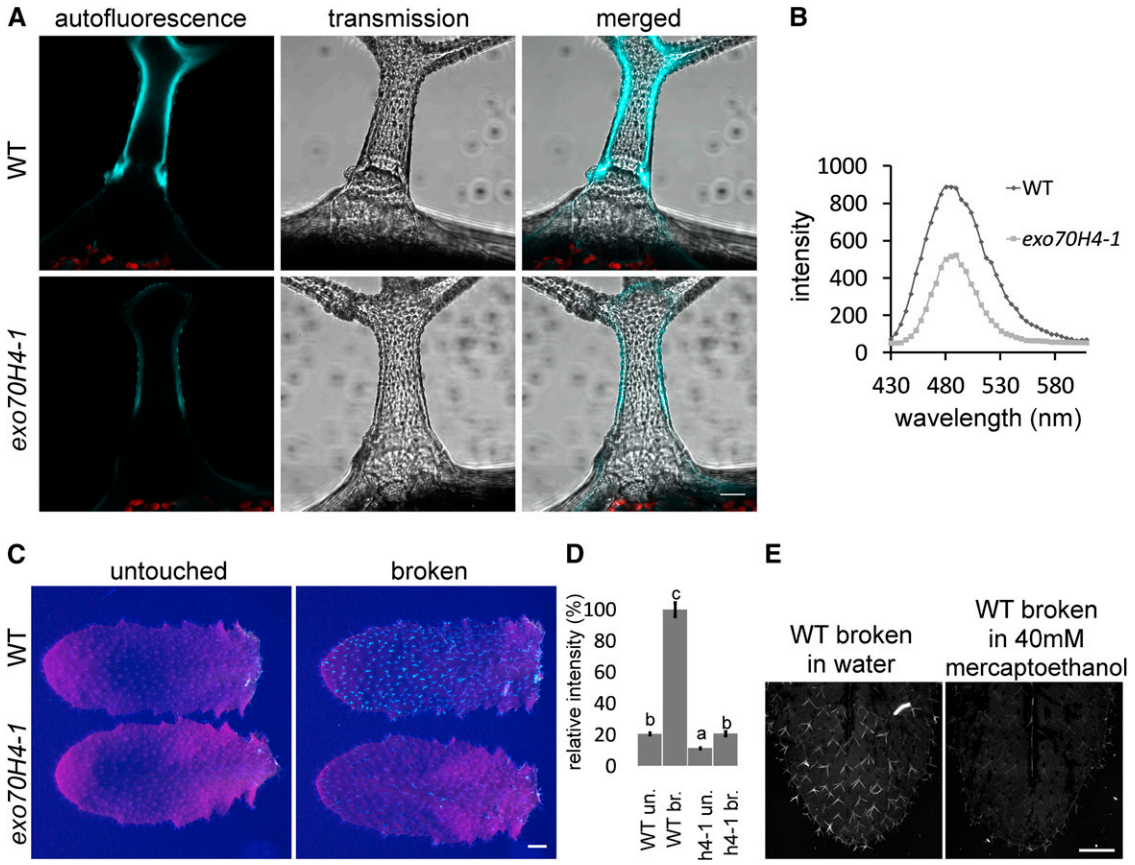

Figure 3. Autofluorescence of the *exo70H4-1* and wild-type (WT) trichomes. A, Autofluorescence of the mature trichome cell wall of wild-type and *exo70H4-1* trichomes. Bar = 20 μm. B, λ-Scan of the trichome autofluorescence reveals a single peak at 485 nm. C, Visualization of the autofluorescence gain after physical damage of trichomes. Bar = 1 mm. D, Quantification of the autofluorescence of the untouched (un.) and broken (br.) trichomes from C. Error bars represent SE. Different letters above bars mean significant differences (HSD Tukey post hoc test, $P < 0.05$). Eighty trichomes per sample were measured. Similar results were obtained from more than three biological replicas. E, Reduction of autofluorescence gain in reducing environment. Bar = 1 mm.

UV-B-Induced EXO70H4 Expression Promotes Cell Wall Thickening and OR Biogenesis

According to several published microarray experiments (Hruz et al., 2008), *EXO70H4* transcription is induced by UV-B irradiation. This induction is, moreover, COP1 dependent, linking expression of EXO70H4 with an already known UV response pathway (Oravecz et al., 2006). However, MeJA (a major regulator of necrotrophic pathogen and herbivore response; Jander and Howe, 2008) inhibits *EXO70H4* transcription (Hruz et al., 2008). Therefore, we have designed experiments to test whether these environmental factors do affect trichome maturation in an EXO70H4-dependent manner.

We have isolated trichomes from fifth and sixth leaves of 24-d-old plants that were treated by UV-B irradiation and/or MeJA for 5 d. Isolated trichomes were then stained with decolorized aniline blue to visualize the OR. As can be seen in Figure 6A, UV irradiation clearly stimulates the callose ring formation, whereas MeJA suppresses it. If both treatments were applied simultaneously, their effects subtracted, resulting in OR abundance similar to in wild-type plants.

We have also examined the effect of UV-B on cell wall thickening in the trichome stalk above the OR. Despite the large defects of cell wall thickening in the trichome apices (Fig. 1C), the differences were rather small but highly significant; UV-B treatment stimulated wild-type thickening by about 10% in contrast to no stimulation in the *exo70H4* mutant. Combined UV and MeJA treatment caused the 10% thickening in both the wild type and *exo70H4*, indicating that this particular mutant phenotype is complemented by an unknown MeJA-dependent mechanism under these combined treatment conditions (Fig. 6B).

Ecophysiological Aspects of Trichome Cell Wall Thickening

Because trichomes have been previously reported to also play a role in anti-herbivore protection, we next asked whether thick secondary walls of wild-type trichomes facilitate plant resistance against insect pests. For this, we performed a weight gain experiment using

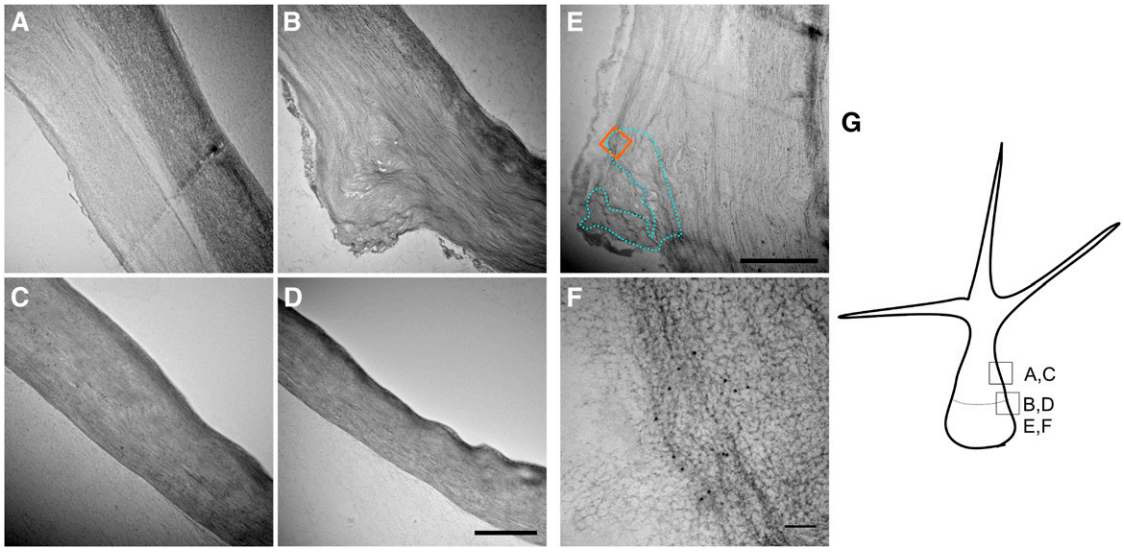

Figure 4. TEM micrographs of wild-type and *exo70H4-1* trichomes. A, Wild-type cell wall above the OR has two distinct layers. B, Wild-type cell wall at the OR. Above the OR, two layers can be recognized, but only one layer is visible beneath the OR. C, *exo70H4-1* cell wall at the place corresponding to A. Only one cell wall layer is visible. D, *exo70H4-1* cell wall at the place corresponding to B. No OR is visible. E, The blue dotted line highlights the region that forms the OR according to the immunogold labeling. The orange square represents the approximate position of F. F, Detail on the immunogold labeling by the anticallose antibody. The position of F is highlighted by the orange square in E. G, Position and orientation of micrographs depicted for better orientation. Bars = 2 μm (A–E) and 100 nm (F).

a specialist herbivore (cabbage butterfly [*Pieris brassicae*]) and a generalist herbivore (Egyptian cotton leafworm [*Spodoptera littoralis*]). First instar caterpillars were placed on both wild-type and *exo70H4* plants for 7 d, after which dry weight gain was measured. For both herbivore species, caterpillars grew less on the *exo70H4* mutants compared with on wild-type plants (Supplemental Fig. S4A). In accordance, we also observed that endogenous MeJA content in *exo70H4* mutants was generally higher than in wild-type plants (Supplemental Fig. S4B). Because jasmonic acid (JA) induction has been linked to increased herbivore resistance in Arabidopsis, we suggest that the influence of trichome stiffness is hazed by other effects, likely MeJA-induced glucosinolate synthesis and overall resistance.

Copper Is Accumulated in the Cell Wall of the OR and above It

Trichomes of other species are well known to accumulate heavy metals, so we were interested if they could be detected in the secondary cell wall and the OR. We have observed second and third true leaves of 24-d-old plants watered by 2 mM $CuSO_4$ and water. Then, copper was stained using dithiooxamide. The copper mainly accumulated in the OR and the cell wall band right above it, whereas it was not detected in the samples watered by regular water. Also, copper was not detected in the *exo70H4-1* mutant, where the whole secondary cell wall is absent (Supplemental Fig. S5).

OR Is Not Likely a Rudiment of Cytokinesis

Arabidopsis trichomes are of unicellular origin; however, DNA endoreduplication suggests their multicellular origin (Hülskamp et al., 1994). In the multicellular trichomes of cucumber, EXO70H4 paralogs are also highly up-regulated (Chen et al., 2014). In these trichomes, the two apical cells also accumulate big amounts of callose, and callose rings are common at the cell divisions (Supplemental Fig. S6).

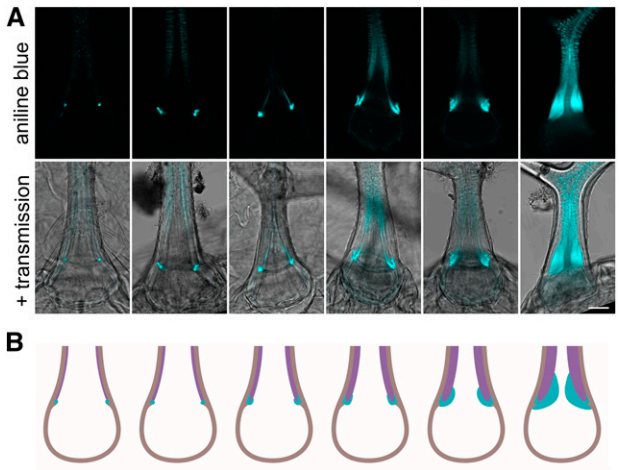

Figure 5. Development of the OR. A, Stages of the trichome maturation accompanied by the secondary cell wall thickening and OR growth. Bar = 20 μm. B, Graphical portrayal of A. Cyan, The OR; purple, the secondary cell wall above the OR; brown, the primary cell wall (respective cellulose-rich cell wall).

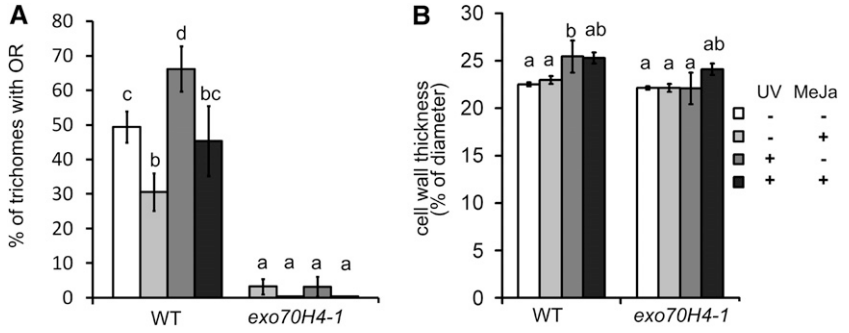

Figure 6. Stimulation of secondary cell wall deposition by UV-B. A, Percentage of trichomes with the OR is increased by the UV and decreased by the MeJA treatment in wild-type (WT) trichomes. B, Relative cell wall thickness of the cell wall in the trichome stalk above the OR. Different letters above bars mean significant differences using the χ^2 test in A ($P < 0.01$) and ANOVA with the HSD Tukey post hoc test ($P < 0.05$) in B. Error bars represent SE. The measurements were made in three biological replicas on more than 20 plants and more than 100 trichomes per treatment and genotype.

Hence, we asked whether Arabidopsis OR is a rudiment of cell plate formation. To address this question, we used the microtubules reporter MICROTUBULE ASSOCIATED PROTEIN4-GFP (MAP4-GFP)-expressing Arabidopsis plant. A band of microtubules distantly resembling a preprophasic band was observed in many trichomes during our observations, and we spotted a correlation between the nucleus position and OR biogenesis (Fig. 7, A–D). Previous studies concluded the final position of the nucleus at the point of the third branching (Hülskamp et al., 1994). We carefully monitored position dynamics of the nucleus in maturing trichomes and realized that, in finally matured/thickened wild-type trichomes, the nucleus, in fact, moved back to basal position. In wild-type trichomes without OR, the nucleus was mostly spotted at the branching point. However, the position of the nucleus was much more basal in the trichomes with OR (Fig. 7, A–C). To test the possibility that OR is a rudiment of cytokinesis, we observed OR in the *Siamese* (*sim*) mutant (GABI_170C01). *SIM* encodes an Interactors of Cdc2 kinase/Kip-related protein cell cycle inhibitor, and mutation in this gene results in ectopic trichome cell divisions (Walker et al., 2000). Surprisingly, these trichomes did not divide in the OR domain (Fig. 7E). Moreover, additional ORs were present in newly divided branches. Hence, this observation did not support the hypothesis that the OR would be a simple rudiment of preprophase or cytokinesis.

DISCUSSION

Here, we show that the final stages of trichome development (i.e. trichome maturation) are characterized by the deposition of an additional layer of the cell wall. Because it is clearly distinguishable and deposited in the last stage of trichome development, we refer to this layer as the secondary cell wall, although biochemical analysis suggested that it has primary wall-like composition (Marks et al., 2008). Strong argument for this cell wall being secondary is the fact that this layer is only formed in the apical part of the trichome and not in the base. The secondary cell wall layer is bordered by a previously undescribed structure, which we propose to name the OR. OR not only borders the secondary cell wall but also, limits the surface papillae distribution, which is much more delimited in the *exo70H4* mutant.

The scenario of OR being a phylogenetic relic of preprophase is unlikely, although our observations do not rule out any other link to the cell cycle. Other phenomena observed can also be explained by different mechanisms. It was shown previously in multiple cases that the nucleus moves toward places with massive secretion (for example, during plant-microbe interactions; Griffis et al., 2014). Also, microtubular structures are often present in active secretory plasma membrane domains, such as the mucilage secretion domain of the outer layer of Arabidopsis seed coat (McFarlane et al., 2008).

OR has been anecdotally spotted before, however, without any additional attention. In figure 1m in Potikha and Delmer (1995), a callose ring was noticed in the trichome, but it was interpreted as a circular wound response. Here, we show that the OR constantly appears with trichome maturation, resulting in nearly 100% of the mature trichomes having the OR. In sum, we propose that, as the trichome maturates, most of its volume is filled up by the callose-rich cell wall, and this thickening is accompanied by the growth of the OR. It should be also noted that callose patterns in the secondary cell wall may vary and are not always as we described here as general pattern. The most common patterns above the OR are small speckles spreading down from the branch tips. Other than the OR, a wide callose band repeatedly appears on the stalk. Interestingly, sometimes not only one OR but two or more are formed. Controlling mechanisms and conditions of these patterns remain unclear and have yet to be studied.

Role of the OR and the Autofluorescent Secondary Cell Wall Layer

The precise role of OR is yet unknown; however, because it borders the autofluorescent and callose-rich inner layer of the cell wall, it likely has a structural

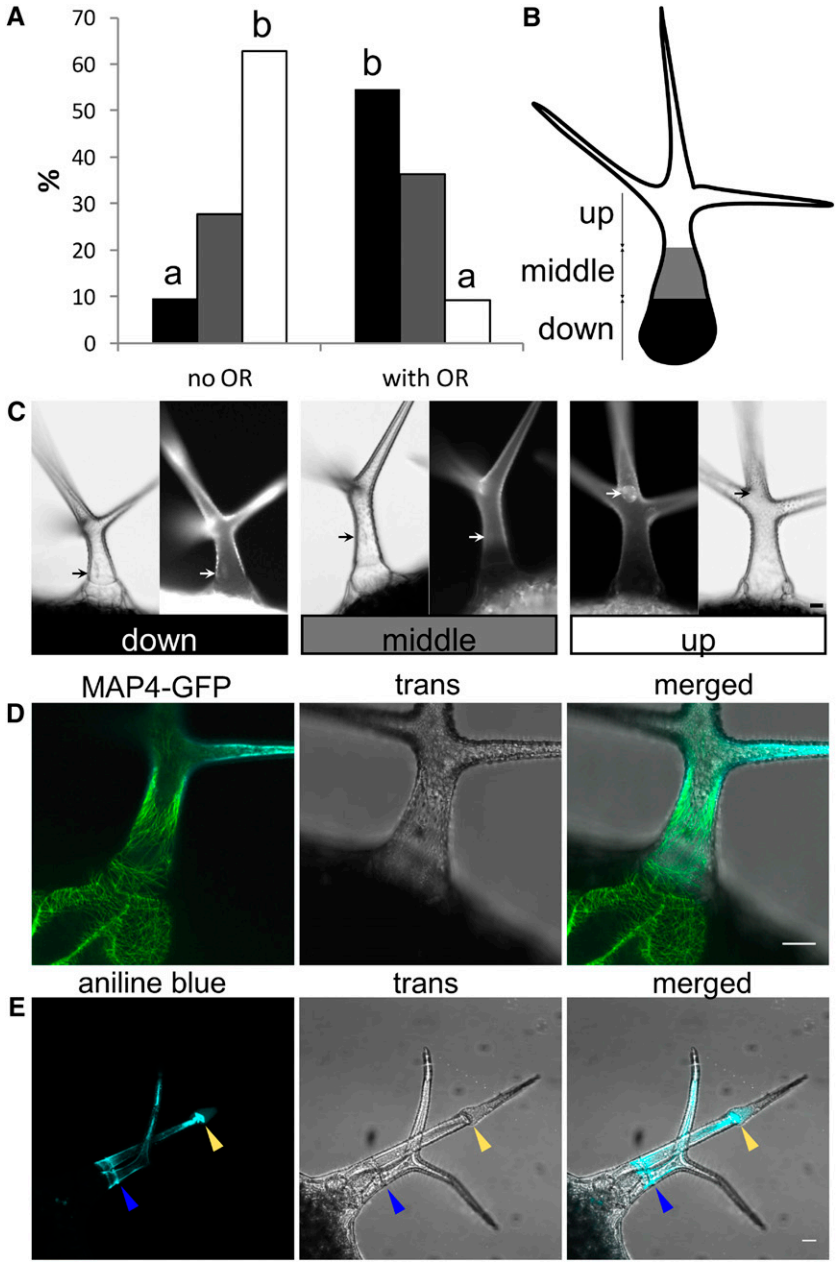

Figure 7. OR biogenesis: link to the nucleus movements and the cell cycle. A, Position of the nuclei in the trichomes before and after the OR formation. Percentage of nuclei located in the lower part of the stalk (black), the middle of the stalk (gray), and the upper part of the stalk (white). Different letters above bars mean significant differences (χ^2 test; $P < 0.0005$); more than 100 trichomes per sample from more than 10 plants were used. Similar results were obtained from three biological replicas. B, Scheme displaying how nucleus position was categorized into three groups. C, Examples of the nucleus (stained by 4′,6-diamino-phenylindole) positions evaluated in A. D, Band of microtubules at the base, which can be spotted before OR biogenesis. E, *sim* mutant ectopic cell divisions (yellow arrow) do not take place at the OR (blue arrow). Bars = 20 μm.

role. The role of the inner layer may be more general and important for many ecophysiological aspects, including UV protection and heavy metal detoxification. Because many toxic compounds, including secondary metabolites, are expected to be deposited in the trichome cell wall, the OR may limit their localization from spreading into other tissues. For example, sequestration of heavy metals in trichomes has been described in both hyperaccumulating and nonaccumulating plant species (Martell, 1974; Salt et al., 1995; Krämer et al., 1997; MacFarlane and Burchett, 1999; Servin et al., 2012; Jr and Kupper, 2014). *Arabidopsis halleri* is a well-known heavy metal hyperaccumulator, with strong evidence for accumulation of zinc, cadmium, and other heavy metals in trichomes. Subcellular localization is in accordance with our results with striking cellular distribution in a narrow ring or thick band at the trichome base (Küpper et al., 2000; Zhao et al., 2000; Sarret et al., 2002; Fukuda et al., 2008), corresponding to the secondary cell wall above the OR. There is also evidence of cadmium hyperaccumulation in trichomes of Arabidopsis (Ager et al., 2002). Jakoby et al. (2008) have shown that zinc transporters and copper chaperones are on the list of the 5% most up-regulated genes in the mature trichome. Hence, the Arabidopsis trichome secondary cell wall may be a permanent storage for toxic heavy metals, which we show here with copper. In this regard, Arabidopsis simple trichomes are analogous to the

glandular trichomes of other species, which also usually have cell wall domains specialized for phytochemical deposition (Turner and Croteau, 2004; Ramirez et al., 2012). Heavy-metal stress has been shown previously to up-regulate the secretory pathway genes in *O. sativa*, including EXO70FX14 and EXO70FX15, which were induced by the copper stress. Similarly, *Nicotiana benthamiana EXO70* is up-regulated by the copper stress and required for the heavy metal-induced reactive oxygen species production (Lin et al., 2013).

We do not yet know the nature of the autofluorescent compounds stored in the trichome secondary cell wall. We have tried multiple lignin stainings, which all gave us negative results, with both healthy and broken trichomes (data not shown).

Interestingly, the whole process of callose accumulation, cell wall thickening, and OR development is enhanced by UV-B irradiation. Trichomes, indeed, play a role in the UV stress response, and their density is increased in plants exposed to UV-B (Yan et al., 2012). UV-B-induced trichome cell wall thickening is in accordance with these results. Induction of EXO70H4 by UV light, resulting in trichome cell wall thickening, indicates a possible function in apical meristem protection against damaging ROS production, although we have not yet performed experiments to confirm this.

The inner trichome cell wall layer also contains a lot of callose, and its absence in *exo70H4* mutants does not cause a change in the trichome birefringence (data not shown). Therefore, the birefringent cell wall layer is likely the outer one, which is also more electron dense on the TEM and contains dense cellulose fibers. This observation is also supported by our CW staining, in which the inner cell wall layer was not stained by the CW in contrast to the *exo70H4* mutant. The presence of ectopic fibrous callose patches in *exo70H4* mutants suggests that callose rather than callose synthase is one of EXO70H4-dependent cargoes. Because the whole internal cell wall layer is callose rich, its development may be callose dependent. Occasional presence of the OR in the *exo70H4* mutant is likely caused by existence of a very close paralog *EXO70H3*, which is a twin gene next to *EXO70H4*, similar to *SEC10a* and *SEC10b* (Vukašinović et al., 2014). *EXO70H3* shows a pollen-specific expression; however, like many other genes, there may be some ectopic expression in the sporophyte. In Arabidopsis pollen, more EXO70 subunits of the H group are expressed, which is probably why *exo70H3* has viable and functional pollen with normal size of the callose plugs (data not shown).

To our surprise, simultaneous application of both UV-B and MeJA induced cell wall thickening in both the *exo70H4* mutant and the wild type without the induction of the OR biogenesis. This may be caused by up-regulation of another EXO70 paralog (for example, EXO70H7, which is stimulated by MeJA on the transcriptional level; Hruz et al., 2008) or another exocyst-independent mechanism.

Because our larval weight experiment did not reveal any importance of *exo70H4*-mediated cell wall thickening for herbivore resistance, we speculate that EXO70H4 is essential for default UV-B-induced thickening, which may be modulated upon herbivore attack. Trichome stiffness itself, however, may still be important to protect against another herbivore species (for example, slugs), and it may be a more general way to improve plant fitness.

Exocyst and Trichome: Questions of the Future Cell Wall Biogenesis Investigation

According to the transcriptomic data (Oravecz et al., 2006; Jakoby et al., 2008), *EXO70H4* is one of the most up-regulated genes in the mature trichome. Surprisingly, this high expression was not noticed in GUS reporter promoter activity assays (Li et al., 2010). This may be because of early observations of too young trichomes combined with very low permeability of old ones.

The EXO70H4 paralog up-regulation in cucumber trichomes (Chen et al., 2014) is a clue that mechanisms of the cell wall thickening in Arabidopsis described here may be a more general phenomenon for land plants that also include multicellular trichome types.

Other (core) exocyst subunits are not dramatically up-regulated in the trichome. Hence, there is a question of the stoichiometry of the complex. Recently, mammalian EXO70 was shown to also function independently from the rest of the exocyst complex in a way analogous to Bin–Amphiphysin–Rvs domain proteins functioning in a membrane deformation (Zhao et al., 2013). We cannot yet exclude the possibility of exocyst-independent function; however, it is worth noting that EXO70H4 interacts with other exocyst subunits in the yeast two-hybrid assays (Supplemental Fig. S2). The stoichiometry question could be explained by post-transcriptional regulation of the EXO70H4 level, which is the case in many other Arabidopsis EXO70s (Stegmann et al., 2012), or possibly, high doses of this subunit are important to compete with the other EXO70s for the rest of the complex, thus modulating its function as proposed in Žárský et al., 2013. Our work aims to answer some of these questions and includes more general analysis of exocyst-dependent callose deposition processes in defense responses.

MATERIALS AND METHODS

Plant Growth and Conditions

T-DNA insertion lines of Arabidopsis (*Arabidopsis thaliana*) were obtained from the Nottingham Arabidopsis Stock Centre (Scholl et al., 2000). These lines were crossed with MAP4-GFP lines (Marc et al., 1998). Plants were grown in Jiffy soil pellets under long-day conditions with illumination of 100 μm m^{-2} s^{-1} photosynthetically active radiation (OSRAM L 58W/930). Plants were planted, placed into paper boxes, and sealed from above by filter foils. Rosco 226 (UV filter) and Rosco 130 (control filter) were used.

Subsequently, plants were exposed to UV-B radiation for 5 d under LT 36W/958 T8 BIOVITAL NARVA fluorescent tubes (which contain UV-B emission peaks) and/or treated with MeJA by installation of slices of filter

papers soaked in the MeJA amount corresponding to a concentration of 0.8 μL L^{-1} box volume (also for 5 d).

In high-light conditions, plants were grown under 700 μm m^{-2} s^{-1} photosynthetically active radiation with Philips HPI-T Plus 400W/645 E40 light bulbs (also with UV-B peak).

Genotype Analysis

The following primers were used for genotyping: *exo70H4-1*, left primer (LP), TGGGATTTCGTTTCACAGTTC and right primer (RP), AATCCGTCATGACGTTGGTAG; exo70H4-3, LP, AACAAACCTGAAGCCATGATG and RP, GTTGCTGTAGTCAGCGAGGAG; Salk LBb 1.3, ATTTTGCCGATTTCGGAAC; GABI_170C01, LP, ATGGATTAACTTGGCATGTGG and RP, TGAAAATGTACTTTTTGGCCAC; and Gabi LB 08409, ATATTGACCATCATACTCATTGC.

The following primers were used for cloning fragments for genomic complementation: EXO70H4 Pst1_for, AAGCTGCAGGCTACAGGAGGCTGGATCATC; and EXO70H4 Kpn1_rev, TCAGGTACCGACATGGATTGCCTTGACCG.

The following primers were used for testing its presence: H4seq3 for, CCGGAGATCATTAATACTAAAA; and TagRFPrev, ATCAACTCTTCACCTTTACTCACCAT.

This fragment has been subcloned into the TagRFP AS-N vector (Evrogen), transferred to the binary vector pBGW (Karimi et al., 2002) by the Clontech LR clonase recombination, and sequenced.

Transcript Detection and Semiquantitative RT-PCR

For detection of transcript in *exo70H4-1* and *exo70H4-3* mutants, RNA was isolated from 100 mg of 7-d-old seedlings grown on Murashige and Skoog plates. RT-PCR was done with the Fermentas First-Strand cDNA Synthesis Kit with 1 μg of total RNA, which was double DNAsed. The following primer pairs were used for transcript detection: GTTTTCCGGCTGCTTGACAT with TATAGCTGCCGGCGAATTGT for the 3′-terminal region and TTTCCATGGTGACGAGAAAAGCAATGAT (forward primer for cloning *EXO70H4* cds) with TATAGCTGCCGGCGAATTGT for the insertion spanning RT-PCR.

Trichome Isolation and Staining

Fifth and sixth leaves were selected from plants (24 d after germination) grown in various conditions (see "Plant Growth and Conditions"). Trichomes were then isolated using a method described in Marks et al. (2008) with minor modifications (phosphate-buffered saline buffer and 100 mM EGTA incubated for 1 h at 50°C).

To stain for the callose, isolated trichomes or whole rosettes were washed for 3 h in acetic acid:ethanol (1:3), washed three times in deionized water, and incubated overnight in aniline blue solution (150 mM KH_2PO_4 and 0.01% [w/v] aniline blue, pH 9.5). This solution without aniline blue was used as a control to check autofluorescence background. For copper staining, after acetic acid-ethanol fixation, samples were washed in 70% (v/v) ethanol and then incubated overnight in a 0.1% (w/v) solution of dithiooxamide in 70% (v/v) ethanol.

Microscopy

Images were acquired with a Leica LCS 510 Confocal Microscope with ×63/1.2 and ×20/0.8 water immersion objectives. A 405-nm laser with an emission window of 470 to 490 nm was used for autofluorescence observation, and a 405-nm laser with an emission window of 490 to 510 nm was used for aniline blue. A 488-nm laser with an emission window of 510 to 530 nm was used for GFP observations. For whole-rosette pictures, a Nikon Eclipse 90i with a ×4 objective was used. Each rosette picture consists of numerous frames that were fused automatically by NIS Elements AR software. Each frame is a maximal projection of three frames with 50 μm of *Z* distance.

TEM and Immunogold Labeling

For TEM, isolated trichomes were fixed for 24 h in 2.5% (v/v) glutaraldehyde in 0.1 M cacodylate buffer (pH 7.2) at 4°C and postfixed in 2% (w/v) OsO_4 in the same buffer. Fixed samples were dehydrated through an ascending ethanol and acetone series and embedded in Epon-Araldite.

On-section immunogold labeling was done using mouse anticallose primary antibody and goat anti-mouse 10-nm golden particles (25128; Aurion) with a standard procedure recommended by the supplier with these conditions: 5% (w/v) bovine serum albumin in phosphate-buffered saline buffer was used as a blocking reagent, and goat monoclonal anti-β-1-3 Glucan from Biosupplies Australia Pty. Ltd. in a concentration 10 μg mL^{-1} was applied for 1 h.

Herbivore Weight Gain Experiments

To measure the specificity of resistance in the Arabidopsis wild type and *exo70H4* mutants, including *exo70H4-1* and *exo70H4-3*, we performed an experiment with two different herbivores: the highly generalist herbivore Egyptian cotton leafworm (*Spodoptera littoralis*; Lepidoptera, Noctuidae) and the cabbage family specialist herbivore cabbage butterfly (*Pieris brassicae*; Lepidoptera, Pieridae). Eggs of Egyptian cotton leafworms were provided by Syngenta, and first instar larvae were obtained by placing eggs at 30°C for 3 d. First instar larvae of cabbage butterflies were provided by Philippe Reymond (University of Lausanne) and obtained from rearing insects on cabbage (*Brassica oleracea*) in controlled greenhouse conditions. All plants were grown in a growth chamber (short days, 20°C, and 55% relative humidity) with a 3:1 mix of commercial potting soil (Orbo-2; Schweizer AG):perlite, and they were 6 weeks old at the time of the experiment. After initial growth, plants were individually surrounded with 330-mL-volume deli plastic cups with the bottoms cut off, and one Egyptian cotton leafworm or one cabbage butterfly larvae (n = 11–13 larvae per herbivore treatment) was added to each plant. Cups were then covered with fine-meshed nylon nets to prevent larvae from escaping, and larvae were allowed to feed for 7 d, after which all surviving larvae were flash frozen in liquid nitrogen, oven dried for 4 d at 50°C, and weighed. An additional four to six plants were set aside, and they were treated in the same way but left herbivore free for measuring constitutive jasmonate production (see below). The main effects of the three different genotypes (the wild type, *exo70H4-1*, and *exo70H4-3*), the two herbivore species (Egyptian cotton leafworm and cabbage butterfly), and their interaction were analyzed with two-way ANOVA.

JA content in leaves was analyzed by collecting one leaf per plant. The extraction was performed by grinding 200 mg of fresh leaves to a powder and mixing with 990 μL of extraction solvent (ethylacetate:formic acid at 99.5:0.5) and 10 μL of internal standards (containing isotopically labeled d5-JA at a concentration of 100 ng mL^{-1}) in a mixer mill at 30 Hz. After centrifugation and evaporation of the supernatant, the residue was resuspended in 100 μL of 70% (v/v) MeOH. Five microliters of solution was injected for ultra-high-performance liquid chromatography-mass spectrometry/mass spectrometry analysis following the same conditions as in Glauser et al. (2014). The final concentration of JA is expressed in nanograms per gram times fresh weight. The main effects of the three different genotypes (the wild type, *exo70H4-1*, and *exo70H4-3*), the herbivore treatment (Egyptian cotton leafworm, cabbage butterfly, and control), and their interaction on JA concentrations were analyzed with two-way permutation ANOVA using the lmPerm package in R (Wheeler, 2010).

Yeast Two-Hybrid Assays

The yeast (*Saccharomyces cerevisiae*) two hybrid was performed as described previously (Hála et al., 2008). We used the Matchmaker GAL4 Two-Hybrid System 3 (Clontech) following the manufacturer's instructions. We used constructs prepared by Hála et al. (2008), Fendrych et al. (2010), and Pecenková et al. (2011), and *EXO70H4* cds was amplified from genomic DNA and subcloned into the pGBKT7 vector between *Nco*I and *Sal*I using these primers: For_EXO70H4_*Nco*I, TTTCCATGGTGACGAGAAAAGCAATGAT; and Rev_EXO70H4_*Sal*I, TTTGTCGACTTAGGACATGGATTGCCTTGAC. From this vector, EXO70H4 cds was recloned into pGADT7 using *Nde*I and *Xho*I restriction sites.

Supplemental Data

The following supplemental materials are available.

Supplemental Figure S1. Genetic complementation of the *exo70H4-1* mutant.

Supplemental Figure S2. Yeast two-hybrid interactions of EXO70H4 and other exocyst subunits.

Supplemental Figure S3. Calcofluor white staining of the wild-type and *exo70H4-1* mutant trichomes.

Supplemental Figure S4. Herbivore studies on *exo70H4* mutants.

Supplemental Figure S5. Copper accumulation in wild-type and *exo70H4-1* trichomes.

Supplemental Figure S6. Callose in the cucumber trichome.

ACKNOWLEDGMENTS

We thank Dr. Miroslav Hyliš for extensive help with the TEM microscopy, Juraj Sekereš for data mining from transcriptomic databases, and Marta Čadyová for technical support.

Received January 24, 2015; accepted March 10, 2015; published March 12, 2015.

LITERATURE CITED

Ager FJ, Ynsa MD, Domínguez-Solís JR, Gotor C, Respaldiza MA, Romero LC (2002) Cadmium localization and quantification in the plant Arabidopsis thaliana using micro-PIXE. Nucl Instrum Methods Phys Res B **189:** 494–498

Bischoff V, Nita S, Neumetzler L, Schindelasch D, Urbain A, Eshed R, Persson S, Delmer D, Scheible WR (2010) *TRICHOME BIREFRINGENCE* and its homolog *AT5G01360* encode plant-specific DUF231 proteins required for cellulose biosynthesis in Arabidopsis. Plant Physiol **153:** 590–602

Brininstool G, Kasili R, Simmons LA, Kirik V, Hülskamp M, Larkin JC (2008) Constitutive Expressor of Pathogenesis-related Genes5 affects cell wall biogenesis and trichome development. BMC Plant Biol **8:** 58

Chen C, Liu M, Jiang L, Liu X, Zhao J, Yan S, Yang S, Ren H, Liu R, Zhang X (2014) Transcriptome profiling reveals roles of meristem regulators and polarity genes during fruit trichome development in cucumber (Cucumis sativus L.). J Exp Bot **65:** 4943–4958

Cole RA, Fowler JE (2006) Polarized growth: maintaining focus on the tip. Curr Opin Plant Biol **9:** 579–588

Cole RA, Synek L, Zarsky V, Fowler JE (2005) SEC8, a subunit of the putative Arabidopsis exocyst complex, facilitates pollen germination and competitive pollen tube growth. Plant Physiol **138:** 2005–2018

Cvrčková F, Grunt M, Bezvoda R, Hála M, Kulich I, Rawat A, Zárský V (2012) Evolution of the land plant exocyst complexes. Front Plant Sci **3:** 159

Ding Y, Wang J, Chun Lai JH, Ling Chan VH, Wang X, Cai Y, Tan X, Bao Y, Xia J, Robinson DG, et al (2014) Exo70E2 is essential for exocyst subunit recruitment and EXPO formation in both plants and animals. Mol Biol Cell **25:** 412–426

Ehleringer J (1982) The influence of water stress and temperature on leaf pubescence development in encelia farinosa. Am J Bot **69:** 670–675

Elias M, Drdova E, Ziak D, Bavlnka B, Hala M, Cvrckova F, Soukupova H, Zarsky V (2003) The exocyst complex in plants. Cell Biol Int **27:** 199–201

Espigares T, Peco B (1995) Mediterranean annual pasture dynamics: impact of autumn drought. J Ecol **83:** 135–142

Fendrych M, Synek L, Pecenková T, Toupalová H, Cole R, Drdová E, Nebesárová J, Sedinová M, Hála M, Fowler JE, et al (2010) The *Arabidopsis* exocyst complex is involved in cytokinesis and cell plate maturation. Plant Cell **22:** 3053–3065

Finger FP, Hughes TE, Novick P (1998) Sec3p is a spatial landmark for polarized secretion in budding yeast. Cell **92:** 559–571

Folkers U, Berger J, Hülskamp M (1997) Cell morphogenesis of trichomes in Arabidopsis: differential control of primary and secondary branching by branch initiation regulators and cell growth. Development **124:** 3779–3786

Fukuda N, Hokura A, Kitajima N, Terada Y, Saito H, Abe T, Nakai I (2008) Micro X-ray fluorescence imaging and micro X-ray absorption spectroscopy of cadmium hyper-accumulating plant, Arabidopsis halleri ssp. gemmifera, using high-energy synchrotron radiation. J Anal At Spectrom **23:** 1068–1075

Glauser G, Vallat A, Balmer D (2014) Hormone profiling. Methods Mol Biol **1062:** 597–608

Grammatikopoulos G, Manetas Y (1994) Direct absorption of water by hairy leaves of Phlomis fruticosa and its contribution to drought avoidance. Can J Bot **72:** 1805–1811

Griffis AHN, Groves NR, Zhou X, Meier I (2014) Nuclei in motion: movement and positioning of plant nuclei in development, signaling, symbiosis, and disease. Front Plant Sci **5:** 129

Hála M, Cole R, Synek L, Drdová E, Pecenková T, Nordheim A, Lamkemeyer T, Madlung J, Hochholdinger F, Fowler JE, et al (2008) An exocyst complex functions in plant cell growth in *Arabidopsis* and tobacco. Plant Cell **20:** 1330–1345

Haughn GW, Somerville CR (1988) Genetic control of morphogenesis in Arabidopsis. Dev Genet **9:** 73–89

He B, Xi F, Zhang X, Zhang J, Guo W (2007) Exo70 interacts with phospholipids and mediates the targeting of the exocyst to the plasma membrane. EMBO J **26:** 4053–4065

Hruz T, Laule O, Szabo G, Wessendorp F, Bleuler S, Oertle L, Widmayer P, Gruissem W, Zimmermann P (2008) Genevestigator v3: a reference expression database for the meta-analysis of transcriptomes. Adv Bioinforma **2008:** 420747

Hülskamp M, Misŕa S, Jürgens G (1994) Genetic dissection of trichome cell development in Arabidopsis. Cell **76:** 555–566

Jakoby MJ, Falkenhan D, Mader MT, Brininstool G, Wischnitzki E, Platz N, Hudson A, Hülskamp M, Larkin J, Schnittger A (2008) Transcriptional profiling of mature Arabidopsis trichomes reveals that *NOECK* encodes the MIXTA-like transcriptional regulator MYB106. Plant Physiol **148:** 1583–1602

Jander G, Howe G (2008) Plant interactions with arthropod herbivores: state of the field. Plant Physiol **146:** 801–803

Karimi M, Inzé D, Depicker A (2002) GATEWAY vectors for Agrobacterium-mediated plant transformation. Trends Plant Sci **7:** 193–195

Krämer U, Grime GW, Smith JAC, Hawes CR, Baker AJM (1997) Micro-PIXE as a technique for studying nickel localization in leaves of the hyperaccumulator plant Alyssum lesbiacum. Nucl Instrum Methods Phys Res B **130:** 346–350

Kulich I, Pečenková T, Sekereš J, Smetana O, Fendrych M, Foissner I, Höftberger M, Zárský V (2013) Arabidopsis exocyst subcomplex containing subunit EXO70B1 is involved in autophagy-related transport to the vacuole. Traffic **14:** 1155–1165

Küpper H, Lombi E, Zhao FJ, McGrath SP (2000) Cellular compartmentation of cadmium and zinc in relation to other elements in the hyperaccumulator Arabidopsis halleri. Planta **212:** 75–84

Li S, van Os GMA, Ren S, Yu D, Ketelaar T, Emons AMC, Liu CM (2010) Expression and functional analyses of *EXO70* genes in Arabidopsis implicate their roles in regulating cell type-specific exocytosis. Plant Physiol **154:** 1819–1830

Liepman AH, Wightman R, Geshi N, Turner SR, Scheller HV (2010) Arabidopsis - a powerful model system for plant cell wall research. Plant J **61:** 1107–1121

Lin CY, Trinh NN, Fu SF, Hsiung YC, Chia LC, Lin CW, Huang HJ (2013) Comparison of early transcriptome responses to copper and cadmium in rice roots. Plant Mol Biol **81:** 507–522

Luo G, Zhang J, Guo W (2014). The role of Sec3p in secretory vesicle targeting and exocyst complex assembly. Mol Biol Cell **25:** 3813–3822

MacFarlane GR, Burchett MD (1999) Zinc distribution and excretion in the leaves of the grey mangrove, Avicennia marina (Forsk.). Vierh Environ Exp Bot **41:** 167–175

Madson M, Dunand C, Li X, Verma R, Vanzin GF, Caplan J, Shoue DA, Carpita NC, Reiter WD (2003) The *MUR3* gene of *Arabidopsis* encodes a xyloglucan galactosyltransferase that is evolutionarily related to animal exostosins. Plant Cell **15:** 1662–1670

Marc J, Granger CL, Brincat J, Fisher DD, Kao Th, McCubbin AG, Cyr RJ (1998) A GFP-MAP4 reporter gene for visualizing cortical microtubule rearrangements in living epidermal cells. Plant Cell **10:** 1927–1940

Marks MD, Betancur L, Gilding E, Chen F, Bauer S, Wenger JP, Dixon RA, Haigler CH (2008) A new method for isolating large quantities of *Arabidopsis* trichomes for transcriptome, cell wall and other types of analyses. Plant J **56:** 483–492

Marks MD, Esch J, Herman P, Sivakumaran S, Oppenheimer D (1991) A model for cell-type determination and differentiation in plants. Symp Soc Exp Biol **45:** 77–87

Marks MD, Wenger JP, Gilding E, Jilk R, Dixon RA (2009) Transcriptome analysis of Arabidopsis wild-type and gl3-sst sim trichomes identifies four additional genes required for trichome development. Mol Plant **2:** 803–822

Martell EA (1974) Radioactivity of tobacco trichomes and insoluble cigarette smoke particles. Nature **249:** 215–217

McFarlane HE, Young RE, Wasteneys GO, Samuels AL (2008) Cortical microtubules mark the mucilage secretion domain of the plasma membrane in Arabidopsis seed coat cells. Planta **227:** 1363–1375

McNear DH Jr, Kupper JV (2014) Mechanisms of trichome-specific Mn accumulation and toxicity in the Ni hyperaccumulator Alyssum murale. Plant Soil **377:** 407–422

Munson M, Novick P (2006) The exocyst defrocked, a framework of rods revealed. Nat Struct Mol Biol **13:** 577–581

Oravecz A, Baumann A, Máté Z, Brzezinska A, Molinier J, Oakeley EJ, Adám E, Schäfer E, Nagy F, Ulm R (2006) CONSTITUTIVELY PHOTOMORPHOGENIC1 is required for the UV-B response in *Arabidopsis*. Plant Cell **18:** 1975–1990

Pecenková T, Hála M, Kulich I, Kocourková D, Drdová E, Fendrych M, Toupalová H, Zársky V (2011) The role for the exocyst complex subunits Exo70B2 and Exo70H1 in the plant-pathogen interaction. J Exp Bot **62:** 2107–2116

Pérez-Estrada LB, Cano-Santana Z, Oyama K (2000) Variation in leaf trichomes of Wigandia urens: environmental factors and physiological consequences. Tree Physiol **20:** 629–632

Potikha T, Delmer DP (1995) A mutant of Arabidopsis thaliana displaying altered patterns of cellulose deposition. Plant J **7:** 453–460

Ramirez AM, Stoopen G, Menzel TR, Gols R, Bouwmeester HJ, Dicke M, Jongsma MA (2012) Bidirectional secretions from glandular trichomes of pyrethrum enable immunization of seedlings. Plant Cell **24:** 4252–4265

Riddick EW, Simmons AM (2014) Do plant trichomes cause more harm than good to predatory insects? Pest Manag Sci **70:** 1655–1665

Salt DE, Prince RC, Pickering IJ, Raskin I (1995) Mechanisms of cadmium mobility and accumulation in Indian mustard. Plant Physiol **109:** 1427–1433

Sarret G, Saumitou-Laprade P, Bert V, Proux O, Hazemann JL, Traverse A, Marcus MA, Manceau A (2002) Forms of zinc accumulated in the hyperaccumulator *Arabidopsis halleri*. Plant Physiol **130:** 1815–1826

Scholl RL, May ST, Ware DH (2000) Seed and molecular resources for Arabidopsis. Plant Physiol **124:** 1477–1480

Servin AD, Castillo-Michel H, Hernandez-Viezcas JA, Diaz BC, Peralta-Videa JR, Gardea-Torresdey JL (2012) Synchrotron micro-XRF and micro-XANES confirmation of the uptake and translocation of TiO_2 nanoparticles in cucumber (Cucumis sativus) plants. Environ Sci Technol **46:** 7637–7643

Stegmann M, Anderson RG, Ichimura K, Pecenkova T, Reuter P, Žársky V, McDowell JM, Shirasu K, Trujillo M (2012) The ubiquitin ligase PUB22 targets a subunit of the exocyst complex required for PAMP-triggered responses in *Arabidopsis*. Plant Cell **24:** 4703–4716

Suo B, Seifert S, Kirik V (2013) Arabidopsis GLASSY HAIR genes promote trichome papillae development. J Exp Bot **64:** 4981–4991

Synek L, Schlager N, Eliás M, Quentin M, Hauser MT, Zársky V (2006) AtEXO70A1, a member of a family of putative exocyst subunits specifically expanded in land plants, is important for polar growth and plant development. Plant J **48:** 54–72

Szymanski DB, Jilk RA, Pollock SM, Marks MD (1998) Control of GL2 expression in Arabidopsis leaves and trichomes. Development **125:** 1161–1171

Szymanski DB, Lloyd AM, Marks MD (2000) Progress in the molecular genetic analysis of trichome initiation and morphogenesis in Arabidopsis. Trends Plant Sci **5:** 214–219

TerBush DR, Maurice T, Roth D, Novick P (1996) The Exocyst is a multiprotein complex required for exocytosis in Saccharomyces cerevisiae. EMBO J **15:** 6483–6494

Turner GW, Croteau R (2004) Organization of monoterpene biosynthesis in Mentha: immunocytochemical localizations of geranyl diphosphate synthase, limonene-6-hydroxylase, isopiperitenol dehydrogenase, and pulegone reductase. Plant Physiol **136:** 4215–4227

Vanzin GF, Madson M, Carpita NC, Raikhel NV, Keegstra K, Reiter WD (2002) The mur2 mutant of Arabidopsis thaliana lacks fucosylated xyloglucan because of a lesion in fucosyltransferase AtFUT1. Proc Natl Acad Sci USA **99:** 3340–3345

Vukašinović N, Cvrčková F, Eliáš M, Cole R, Fowler JE, Žársky V, Synek L (2014) Dissecting a hidden gene duplication: the Arabidopsis thaliana SEC10 locus. PLoS ONE **9:** e94077

Walker JD, Oppenheimer DG, Concienne J, Larkin JC (2000) SIAMESE, a gene controlling the endoreduplication cell cycle in Arabidopsis thaliana trichomes. Development **127:** 3931–3940

Wang J, Ding Y, Wang J, Hillmer S, Miao Y, Lo SW, Wang X, Robinson DG, Jiang L (2010) EXPO, an exocyst-positive organelle distinct from multivesicular endosomes and autophagosomes, mediates cytosol to cell wall exocytosis in *Arabidopsis* and tobacco cells. Plant Cell **22:** 4009–4030

Wang S, Yin Y, Ma Q, Tang X, Hao D, Xu Y (2012) Genome-scale identification of cell-wall related genes in Arabidopsis based on co-expression network analysis. BMC Plant Biol **12:** 138

Wheeler RE (2010) multResp(lmPerm). The R Project for Statistical Computing. http://www.r-project.org/ (January 14, 2015)

Yamasaki S, Noguchi N, Mimaki K (2007) Continuous UV-B irradiation induces morphological changes and the accumulation of polyphenolic compounds on the surface of cucumber cotyledons. J Radiat Res (Tokyo) **48:** 443–454

Yan A, Pan J, An L, Gan Y, Feng H (2012) The responses of trichome mutants to enhanced ultraviolet-B radiation in Arabidopsis thaliana. J Photochem Photobiol B **113:** 29–35

Zársky V, Cvrcková F, Potocký M, Hála M (2009) Exocytosis and cell polarity in plants - exocyst and recycling domains. New Phytol **183:** 255–272

Zársky V, Kulich I, Fendrych M, Pečenková T (2013) Exocyst complexes multiple functions in plant cells secretory pathways. Curr Opin Plant Biol **16:** 726–733

Zhao FJ, Lombi E, Breedon T, McGrath SP (2000) Zinc hyperaccumulation and cellular distribution in *Arabidopsis halleri*. Plant Cell Environ **23:** 507–514

Zhao Y, Liu J, Yang C, Capraro BR, Baumgart T, Bradley RP, Ramakrishnan N, Xu X, Radhakrishnan R, Svitkina T, et al (2013) Exo70 generates membrane curvature for morphogenesis and cell migration. Dev Cell **26:** 266–278